

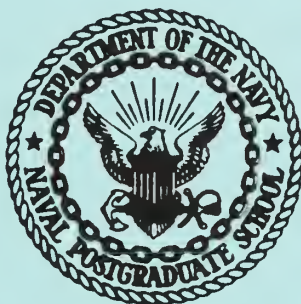
NPS ARCHIVE
1969
LESEMANN, D.

COMPARISONS BETWEEN RADIATION HARDENED
AND STANDARD INTEGRATED CIRCUIT
AMPLIFIERS IN AN ELECTRON BEAM

by

Donald Frederick Lesemann

UNITED STATES NAVAL POSTGRADUATE SCHOOL



THESIS

COMPARISONS BETWEEN RADIATION HARDENED
AND STANDARD INTEGRATED CIRCUIT
AMPLIFIERS IN AN ELECTRON BEAM

by

Donald Frederick Lesemann

April 1969

*This document has been approved for public re-
lease and sale; its distribution is unlimited.*

LIBRARY
U.S. NAVAL POSTGRADUATE SCHOOL
MONTEREY CALIFORNIA

COMPARISONS BETWEEN RADIATION HARDENED AND STANDARD
INTEGRATED CIRCUIT AMPLIFIERS IN AN ELECTRON BEAM

by

Donald Frederick Lesemann
Lieutenant, United States Navy
B.S., California State Polytechnic College, 1962

Submitted in partial fulfillment of the
requirements for the degree of

MASTER OF SCIENCE IN ELECTRICAL ENGINEERING

from the

NAVAL POSTGRADUATE SCHOOL
April 1969

NPS ARCHIVE ~~SECRET~~

1969

LESEMANN, D.

ABSTRACT

An investigation into the effect of radiation from a linear accelerator on two types of integrated circuit operational amplifiers was made. Dielectric isolation, thin film resistors and compensation diodes were used in one amplifier (μ A744). The other amplifier (μ A709) was fabricated using standard methods.

The μ A744 amplifier, in its current stage of development, was found to be more susceptible to the effects of accumulated dose from high energy electrons than the μ A709 amplifier.

TABLE OF CONTENTS

Section	Page
I Introduction	9
II Electron Beam Interaction in Silicon	10
A Ionization	10
B Radiation	11
III Fairchild μ A709 and μ A744 Operational Amplifiers	13
IV Test Procedures and Equipment	20
A Transient	20
B Permanent	20
C Positioning	22
V Results	23
VI Conclusions and Recommendations	42
VII Appendix 1 Dosimetry	44

LIST OF ILLUSTRATIONS

Figure		Page
1	Energy Loss per Centimeter vs. Energy due to Ionization	11
2	Energy per Energy Interval vs. Energy for Photons Produced by Bremsstrahlung	12
3	Schematic Diagram of μ A709 Amplifier	13
4	Schematic Diagram of μ A744 Amplifier	15
5	Dielectric Isolation After Steps (1) and (2)	16
6	Dielectric Isolation After Step (3)	16
7	Dielectric Isolation After Step (4)	16
8	Dielectric Isolation After Step (5)	16
9	Dielectric Isolation After Step (6)	17
10	Dielectric Isolation After Step (7)	17
11	Dielectric Isolation After Step (8)	17
12	Photomicrograph of μ A709 and a μ A744	18
13	Schematic Diagram of Test Circuitry	21
14	Diagram of Test Box	21
15	Transient Response of μ A709 Amplifier	25
16	Transient Response of μ A744 Amplifier	25
17	Gain vs. Dose for μ A744 at 10^{10} rads/sec	27
18	I_{bav} vs. Dose for μ A744 at 10^{10} rads/sec	28
19	Gain vs. Dose for μ A709 at 10^{10} rads/sec	29
20	I_{bav} vs. Dose for μ A709 at 10^{10} rads/sec	30
21	Gain vs. Dose for μ A744 at 10^8 rads/sec	31
22	I_{bav} vs. Dose for μ A744 at 10^8 rads/sec	32
23	Gain vs. Dose for μ A709 at 10^8 rads/sec	33

Figure		Page
24	I_{bav} vs. Dose for μ A709 at 10^8 rads/sec	34
25	Gain vs. Dose for μ A744 at 10^{10} rads/sec	35
26	I_{bav} vs. Dose for μ A744 at 10^{10} rads/sec	36
27	Gain vs. Dose for μ A709 at 10^{10} rads/sec	37
28	I_{bav} vs. Dose for μ A709 at 10^{10} rads/sec	38
29	Gain vs. Measurement Number for Controls	39
30	I_{bav} vs. Measurement Number for Controls	40
31	Sample Data Sheet	41
32	Beam Profile	44

ACKNOWLEDGEMENTS

The assistance of Professors John Dyer and Shu-gar Chan throughout this study is greatly appreciated. Special mention is made of Professors Franz Bumiller and Fred Buskirk for their cooperation and for the use of the linear accelerator.

The personnel of the Linear Integrated Circuits Section of Fairchild Semiconductors Research and Development Laboratory, particularly Ken Stafford, have been especially helpful during this study.

I. INTRODUCTION

The purpose of this study is to investigate the behavior of integrated circuit operational amplifiers in a transient radiation environment. In particular, this investigation makes a comparison between two similar amplifiers. One of these amplifiers was manufactured according to some of the more generally accepted radiation hardening techniques, and the other was fabricated by the normal process.

Radiation resistant circuitry is important primarily to the military in such applications as ballistic missiles, navigation satellites, and communication satellites, but should also be of interest to commercial users.

An electronic circuit may be subjected to basically two types of radiation environment, the high intensity short duration pulse from a nuclear burst and the low intensity long term radiation from space sources or nuclear burst residue. This study deals (directly) only with the effect due to the short duration pulse.

By the use of a lower intensity pulse, which is repeated many times, results similar to exposure for long durations to a constant low level source can be obtained.

II. ELECTRON BEAM INTERACTIONS IN SILICON

The high energy electrons (80-90 Mev for this study) from a linear accelerator interact with matter by ionization and radiation.¹

A. IONIZATION

Incident high energy electrons interact with the atomic electrons to cause ionization. A graph showing the energy loss per centimeter of the incident electron due to this effect, as a function of energy,² is shown in Figure 1. From this graph it can be seen that the ionization loss is reasonably independent of beam energy. The energy that is lost, due to ionization, is deposited in the target material in the form of low energy electrons. These electrons form the photocurrents in an integrated circuit exposed to the electron beam. (The incident electron passes through the target with very little loss of energy).

The common unit for energy deposited in a material (absorbed dose) is the rad, which is defined as 100 ergs per gram. The dose rate can be calculated from

$$\frac{\text{rads}}{\text{sec}} = \left(\frac{1}{\rho} \frac{dE}{dx} \right)_i \phi (1.6 \times 10^{-8})$$

where ϕ is the flux, which is explained more fully in Appendix 1, $\frac{dE}{dx}$ is the energy loss due to ionization, and ρ is the density (gm/cm^3).

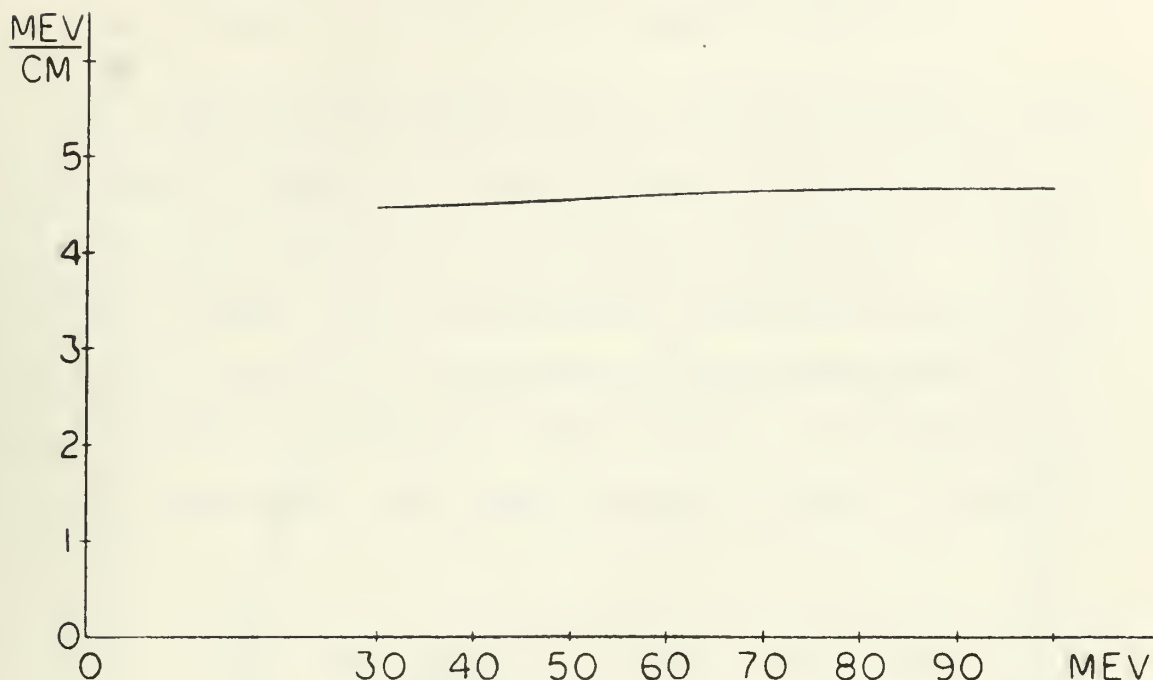


Figure 1. Energy Loss per Centimeter vs.
Energy Due to Ionization

B. RADIATION

Incident high energy electrons also produce radiation (bremsstrahlung) by interaction with target nuclei. For silicon, at about 80 Mev, the energy loss due to this radiation is comparable to the ionization loss. The photons have a spectrum of energies as shown in Figure 2. Nearly all of these photons have mean free paths much greater than the thickness of an integrated circuit chip. As an example, a photon produced with an energy of 1 Mev has a mean free path of several centimeters. This mean free path increases with energy. This means that only those photons with a very small energy would remain in an integrated circuit and be able to cause circuit disturbances. Thus $\left(\frac{1}{\rho} \frac{dE}{dx} \right)_r$ the energy loss due to bremsstrahlung is neglected when calculating the absorbed dose of the circuits.

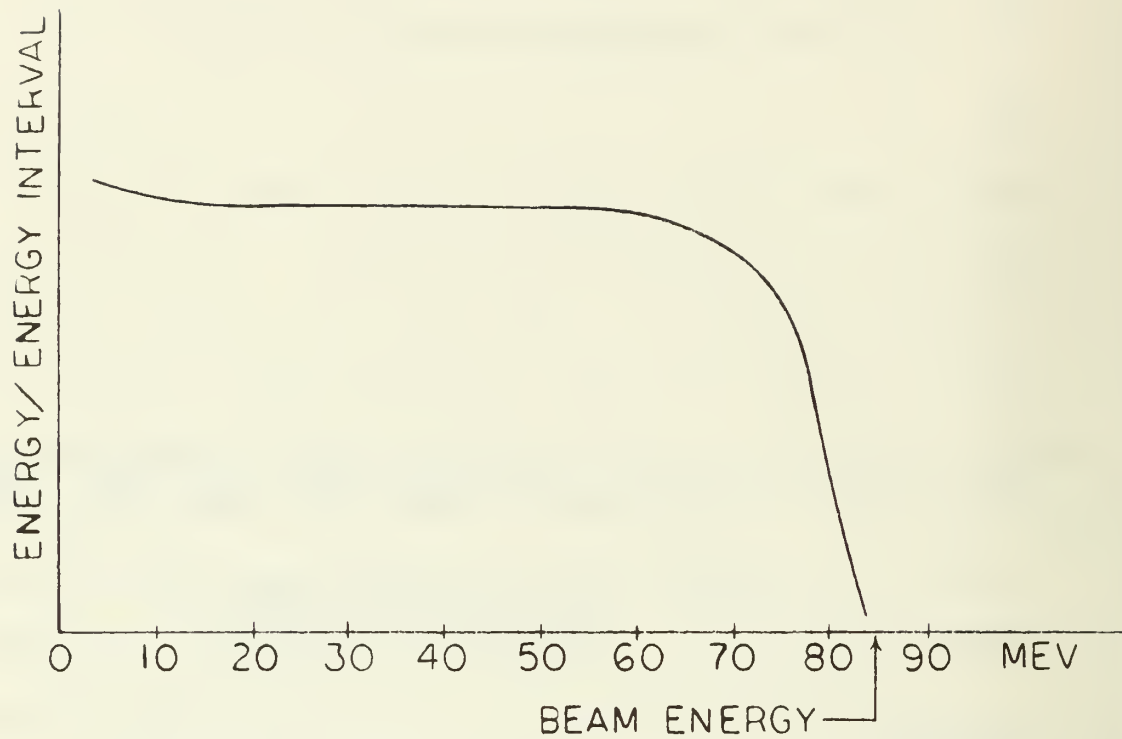


Figure 2 Energy per Energy Interval vs. Energy for Protons
Produced by Bremsstrahlung

III. FAIRCHILD μ A709 AND μ A744 OPERATIONAL AMPLIFIERS

The μ A709 operational amplifier is a standard high gain integrated circuit amplifier which is in common use today. The usual methods of integrated circuit fabrication are used in its manufacture. It features low offset voltages, high input impedance, high output swing under load and low power consumption. It is used in various applications, such as DC servo systems, high impedance analog computers, and low-level instrumentation applications. The schematic diagram is shown in Figure 3.

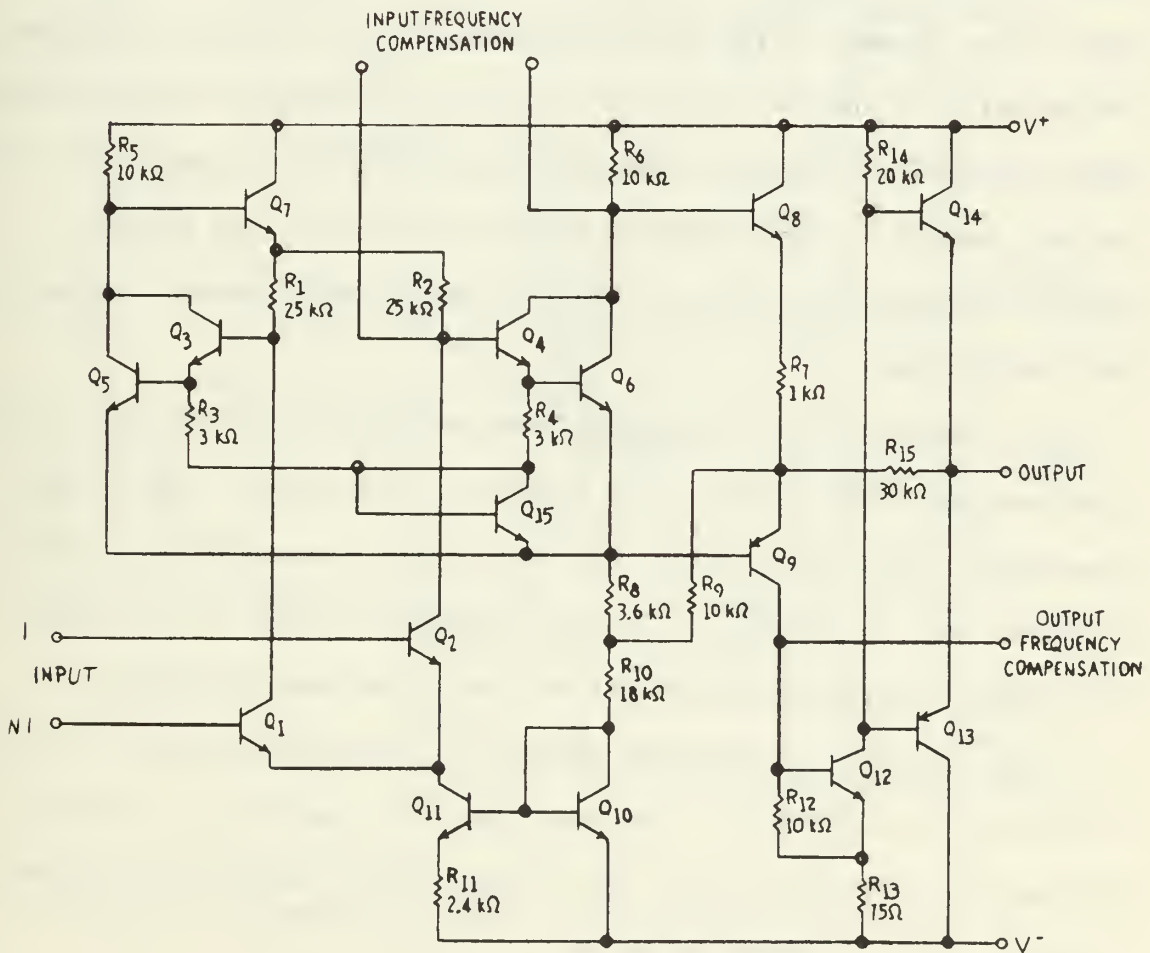


Figure 3. Schematic Diagram of μ A709 Amplifier.

The μ A709 can be divided into three stages³. They are the input, second and output stages.

The input stage is operated at low collector currents and utilizes the difference in the emitter-base voltage of two identical transistors operating at different collector currents to form the current source. With this configuration only low values of resistance (a few thousand ohms) are required. Referring to the schematic (Figure 3), transistors Q_1 and Q_2 form the differential input stage while transistors Q_{11} and Q_{10} form the current source.

The second stage uses a modified Darlington connection which is used to prevent loading of the input stage. The same type of current source that is used in the first stage is utilized again in this stage. The actual amplifier is transistor Q_6 , with Q_5 providing balanced biasing. Other features of this stage are an emitter-follower, Q_7 , which is used to keep the input stage collector currents out of Q_5 , and another emitter-follower, Q_8 , which is used to prevent second stage loading by the output stage.

In transition from the second stage with differential input to the single-ended output stage, level shifting is necessary. This is accomplished with a lateral PNP, Q_9 , which feeds a complementary class-B output pair, Q_{14} and Q_{13} . Internal feedback through R_{15} provides a low output resistance and greatly reduces cross-over distortion.

Two frequency compensation points are provided to enable the use of external R-C networks. This compensation is necessary to prevent the amplifier from going into oscillation, and to provide the desired frequency roll-off characteristics.

The μ A744 is essentially the same amplifier as the μ A709 except for an attempt at radiation hardening. The radiation hardening⁴ is accomplished by dielectric isolation, the use of thin film resistors, and compensating diodes in some critical paths in the circuit. The circuit diagram is shown in Figure 4.

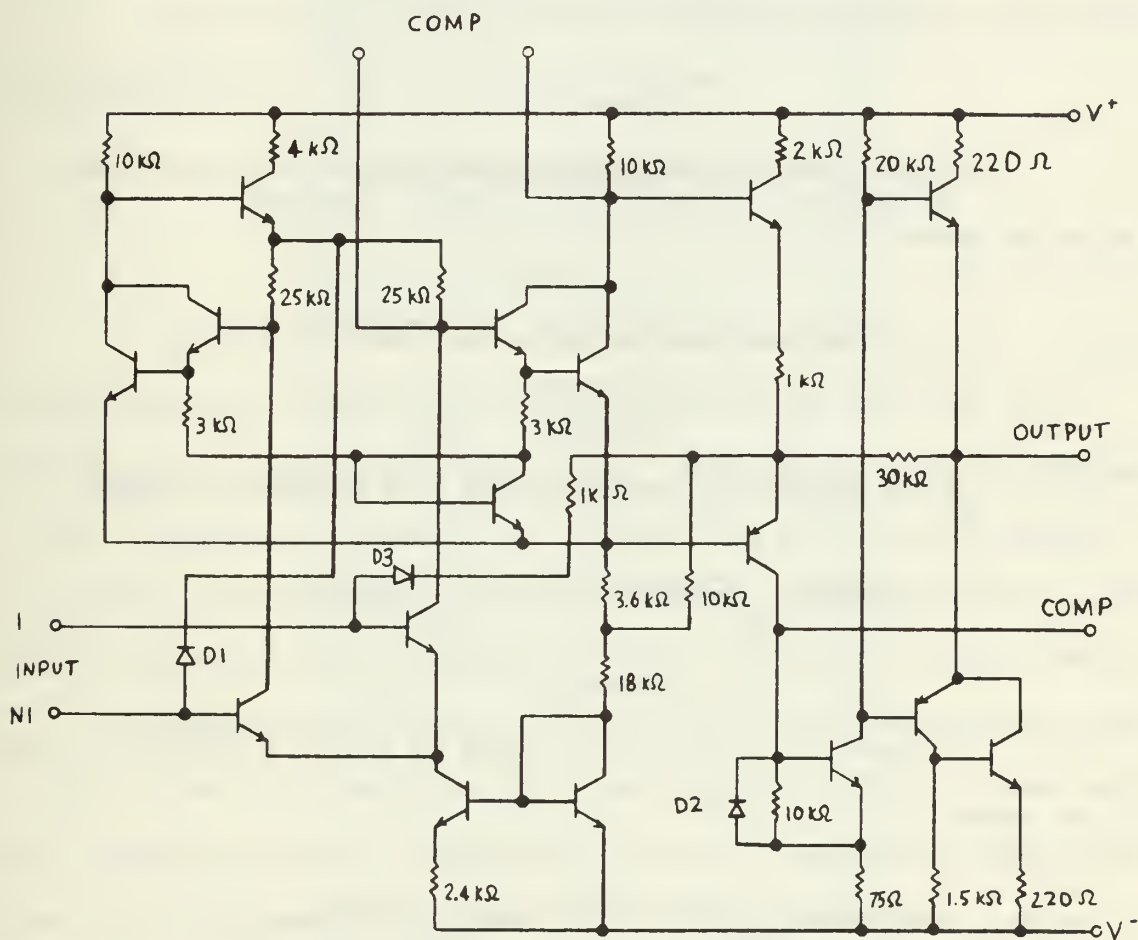


Figure 4. Schematic Diagram of μ A744 Amplifier

Dielectric isolation is a manufacturing technique which enables each transistor (or some small portion of the circuit) to be formed in a pocket which is completely surrounded by silicon-dioxide.

One commonly used process is as follows:⁵ (As illustrated in Figures 5-11).

(1) An epitaxial layer of N⁺ is grown on a N⁻ wafer.

(2) A layer of oxide is grown over the N⁺.

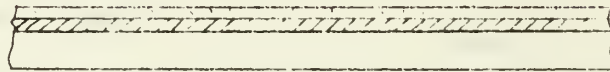


Figure 5

(3) Using photo masking and etching, trenches are cut into the oxide layer.

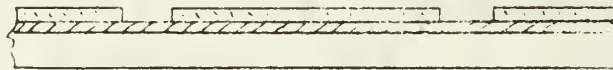


Figure 6

(4) The silicon is then etched to form channels or moats.

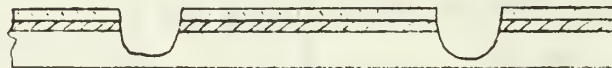


Figure 7

(5) Oxide is regrown on the wafer to coat the interior surfaces of the channels.



Figure 8

(6) Polycrystalline silicon is grown over this oxide to form a rigid support for the circuit.

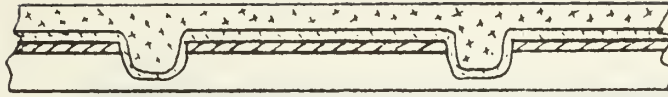


Figure 9

(7) The N- side of the wafer is lapped down to the oxide channels and inverted.

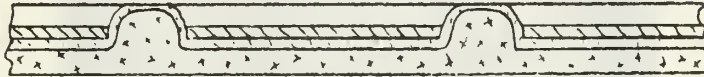


Figure 10

(8) A layer of SiO_2 is grown over the surface; then the circuit is diffused into the chip by standard methods.

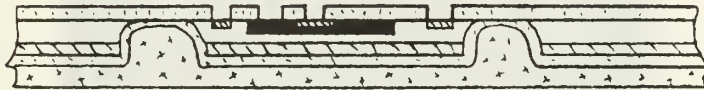
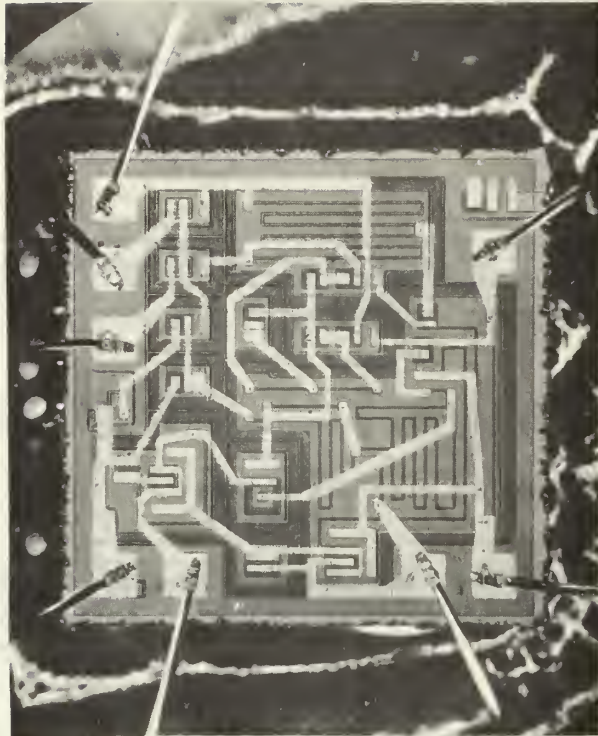


Figure 11

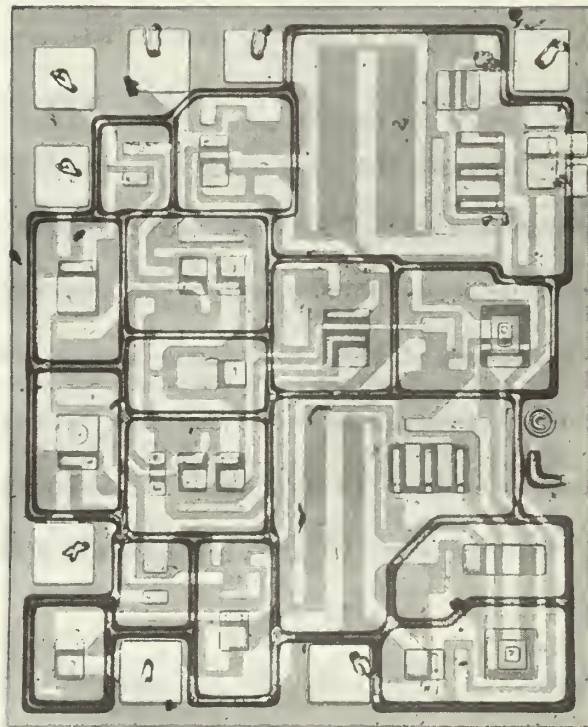
(9) Metalization is applied to complete the process. If care is not exercised during the metalization, small "micro-cracks" may develop due to steps in the oxide layer. These steps occur in integrated circuit fabrication because of the photomasking and diffusion sequence required to form the components. If these small cracks do develop, they will not withstand much heating before they open and the circuit fails.

In a radiation environment this technique should provide much better isolation than the normal reverse biased junction technique. With ionizing radiation present, a normal PN junction is essentially shorted, thus providing no effective isolation. Figure 12 shows a photomicrographic comparison of a μ A709 and a μ A744 die.

The added compensation diode, D_2 , in the μ A744 circuit (Figure 4) will act as a bypass for some of the photocurrent to reduce disturbance of the biasing of the associated transistor. This should enable



μ A709



μ A744

Figure 12 Photomicrographs of μ A709 and μ A744

the circuit to operate properly at a slightly higher exposure rate than the μ A709.

During a high level ionizing radiation pulse, and for some time after it, the component junctions are short-circuited due to the large photo-currents. Thin film resistors, which are capable of supporting the full supply load for times which are long compared to the pulse duration, are used to protect the metalization and components. These resistors can be seen on the photomicrograph of the μ A744 die as large rectangular strips.

IV. TEST PROCEDURES AND EQUIPMENT

The direct electron beam of the linear accelerator at the Naval Postgraduate School, Monterey, California, was the source of ionizing radiation for this study. This is a 100 Mev machine, capable of providing dose rates up to about 10^{10} rads/sec (Si).

The experiments performed can be separated into two major classifications; the transient behavior of the circuit during and after a 1 microsecond pulse of electrons, and the permanent changes in device characteristics as a function of accumulated absorbed dose.

A. TRANSIENT

The test circuit for the transient conditions is shown in Figure 13. This circuitry was located in an aluminum box (Figure 14) with sockets on the top to accept either a μ A709 or a μ A744 mounted on a circuit board, and cable connections for the supply voltages and output signal. The output was monitored remotely on a Tektronix 556 oscilloscope equipped with a Polaroid camera.

B. PERMANENT

For the static tests the operational amplifier was operated with normal bias, but was placed in a positioning device which made it possible to change circuits without going into the target room of the accelerator. The positioning device is designed to hold eleven circuits which can be rotated into the beam line remotely. Through a pair of commutating relays the socket which is connected to the external cables can be selected.⁶

The test circuits used were electrically tested, before and after irradiation, at Fairchild Semiconductors' Research and Development Laboratory in Palo Alto.

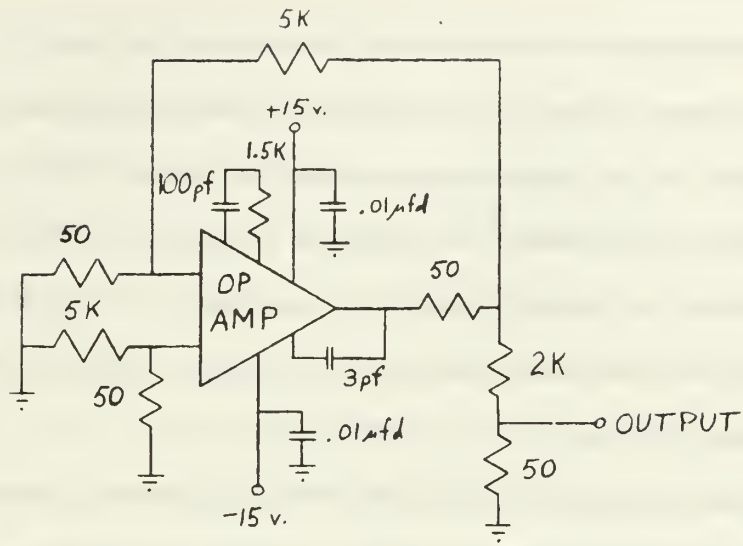


Figure 13. Schematic Diagram of Test Circuitry

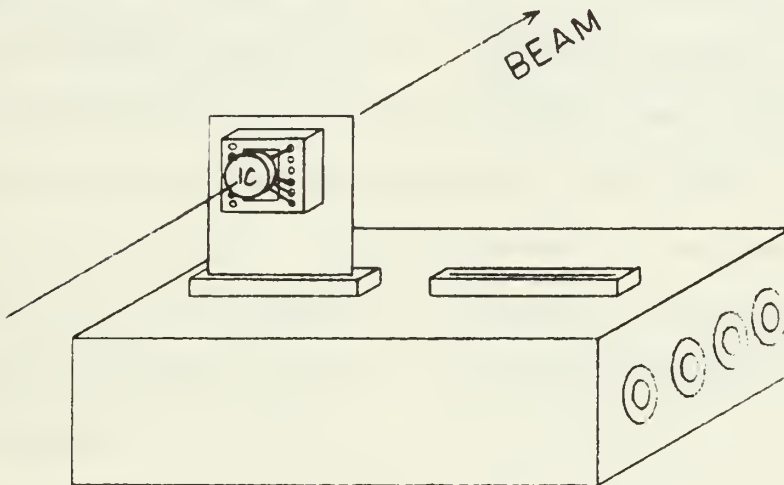


Figure 14. Diagram of Test Box

C. POSITIONING

The integrated circuit die is much smaller than the diameter of the electron beam. There is a spatial distribution of the beam (see Appendix 1), so that it is important to position the circuit in the beam center.

Remote positioning⁶ in both the vertical and horizontal direction is possible. A crossed pair of wires placed in the beam line and monitored with an oscilloscope, and visual alignment using a television camera were used as position indicators.

By use of these techniques, the integrated circuits can be positioned in the center of the beam with an accuracy of about 1mm.

V. RESULTS

Data for the transient tests were taken in the form of Polaroid pictures. Three samples of each type of circuit were exposed at dose rates from 10^8 to 10^{10} (rads/sec) on a single pulse basis. Using this procedure the circuit response to a high dose rate could be observed without accumulating much total dose. Figure 15 shows a typical response of a μ A709. The typical response of a μ A744 is shown in Figure 16. The differences in the responses probably occur because the μ A709 has a common substrate while the μ A744 does not. This means that the two devices would have different current paths so should exhibit different transient characteristics. The sharp changes in the response of the μ A744 are attributed to the recovery of successive stages.

Note that the circuits take from 8 - 14 microseconds to recover from the one microsecond electron pulse. This recovery time is important if a turn-off type of protection device is used. Some μ A709 and μ A744 circuits were exposed with the bias power supply turned off, and also with the (+ 15 v.) supply terminals grounded. It was found that a low level (1.6 - 4.0 v.) transient was produced in the unbiased devices and essentially no transient produced in the devices with the power supply leads grounded.

The circuits for the permanent damage studies were divided into six groups as shown in Table 1. Groups III and VI were used to see if there was any error involved in the successive exposures of groups I, II, IV, V. This error could occur because of normal annealing of the circuits between runs and/or because of accumulated dosimetry error. This did not prove to be a problem, as can be seen by comparing Figures 25, 26, 27, and 28 with Figures 17, 18, 19, and 20 respectively.

The circuit data were recorded by Fairchild Semiconductor Research and Development Laboratory personnel. A sample data sheet is shown in Figure 31. It was decided that of the parameters measured, gain and average input base current would best indicate the circuit condition. The gain is a direct indication of overall circuit performance, particularly the second and output stages. The average base current shows the condition of the input stage.

Figures 17 through 28 show the plots of these parameters versus accumulated dose for each circuit tested. The solid line across each graph indicates the minimum acceptable limit according to the manufacturers' specifications.

A comparison between Figure 17 and Figure 19 shows that the radiation hardened version (μ A744) experienced marked degradation sooner (at a lower accumulated dose) than the non-radiation hardened version (μ A709).

The fact that the μ A744 has larger area input transistors than the μ A709, would seem to offer a good explanation for this result. It can be seen from the average base current plots that the input stage of the μ A744 is affected by accumulated dose more than the input stage of the μ A709. This is not a conclusive proof, however, since the gain of the μ A744s also degrades sooner than that of the μ A709s. This indicates that the interior stages of the μ A744 are more vulnerable than those of the μ A709. This might be due to changes in the fabrication techniques of the μ A744 necessitated by the use of thin film resistors and dielectric isolation.

Groups II and V were exposed at a rate one hundred times less than Groups I and IV. It can be seen from Figures 17-24 that there is little dependence, in the degradation of the circuits, on dose rate.

Fairchild Semiconductor fabricated some special circuits such that individual components could be studied. These circuits (kit-parts) are the same as the normal amplifiers except that the final wiring mask is not used and representative individual components are brought out to the circuit leads.

Two samples of each type of kit parts were exposed to the beam at a rate of 10^{10} rad/sec to a dose of 10^7 rads. They were then tested at Fairchild to see if one type of component was showing more degradation than the others. These tests showed that there was no appreciable difference in the degradation of the corresponding types of components in the two circuits.

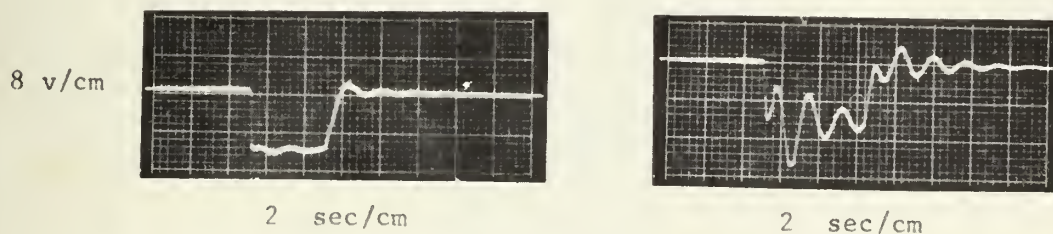


Figure 15. Transient Response of μ A709 Amplifier.

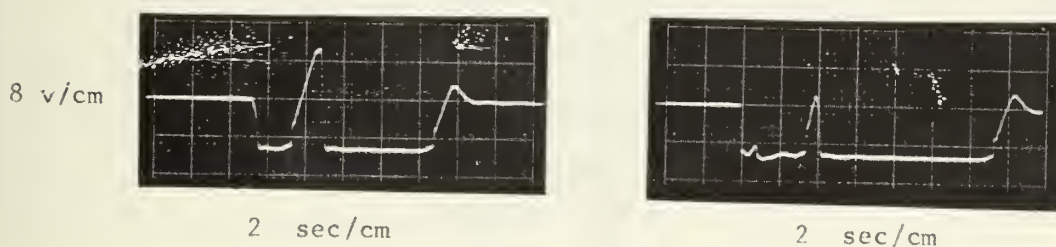
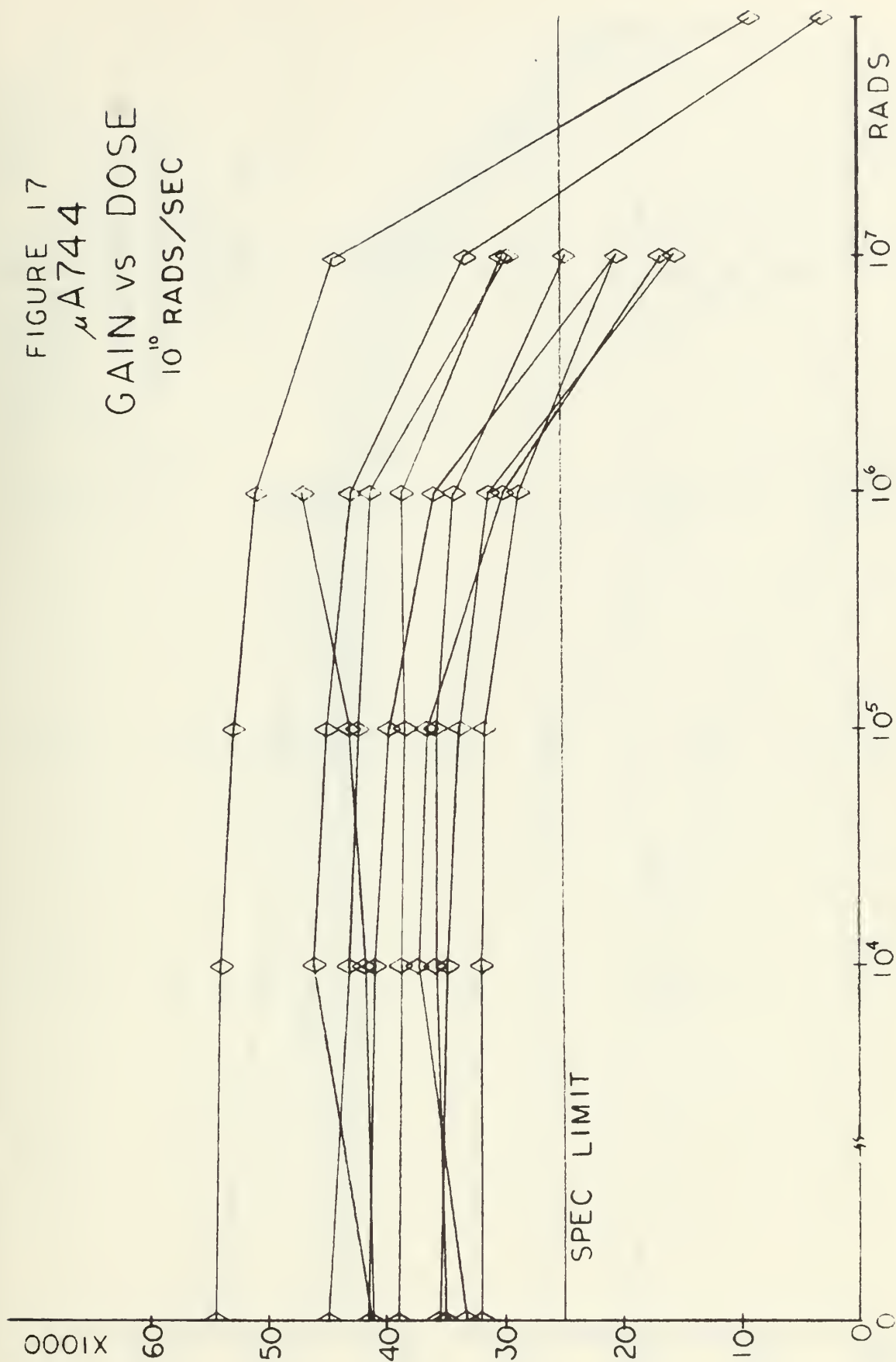


Figure 16. Transient Response of μ A744 Amplifier.

TABLE I

Group #	Type	Exposure Rate	Exposure History	Figure #
I	μ A744	10^{10} rads/sec	$0, 10^4, 10^5, 10^6, 10^7, 10^8$	17, 18
II	μ A744	10^8 rads/sec	$0, 10^4, 10^5, 10^6, 10^7$	21, 22
III	μ A744	10^{10} rads/sec	$0, 10^6$	25, 26
IV	μ A709	10^{10} rads/sec	$0, 10^4, 10^5, 10^6, 10^7, 10^8$	19, 20
V	μ A709	10^8 rads/sec	$0, 10^4, 10^5, 10^6, 10^7$	23, 24
VI	μ A709	10^{10} rads/sec	$0, 10^6$	27, 28
Controls	μ A744, μ A709		None	29, 30

FIGURE 17
 μ A744
 GAIN vs DOSE
 10^{10} RADS/SEC



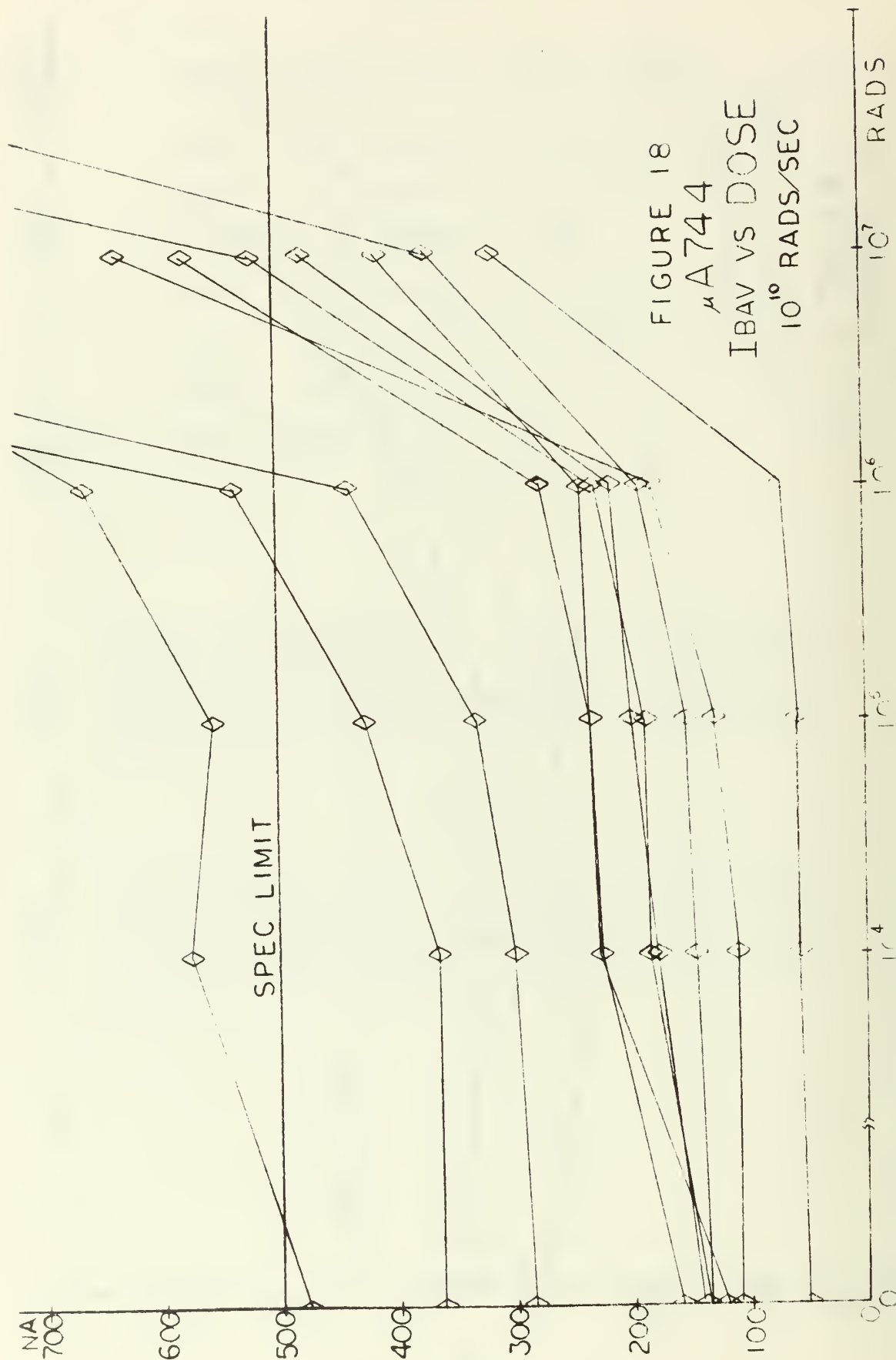
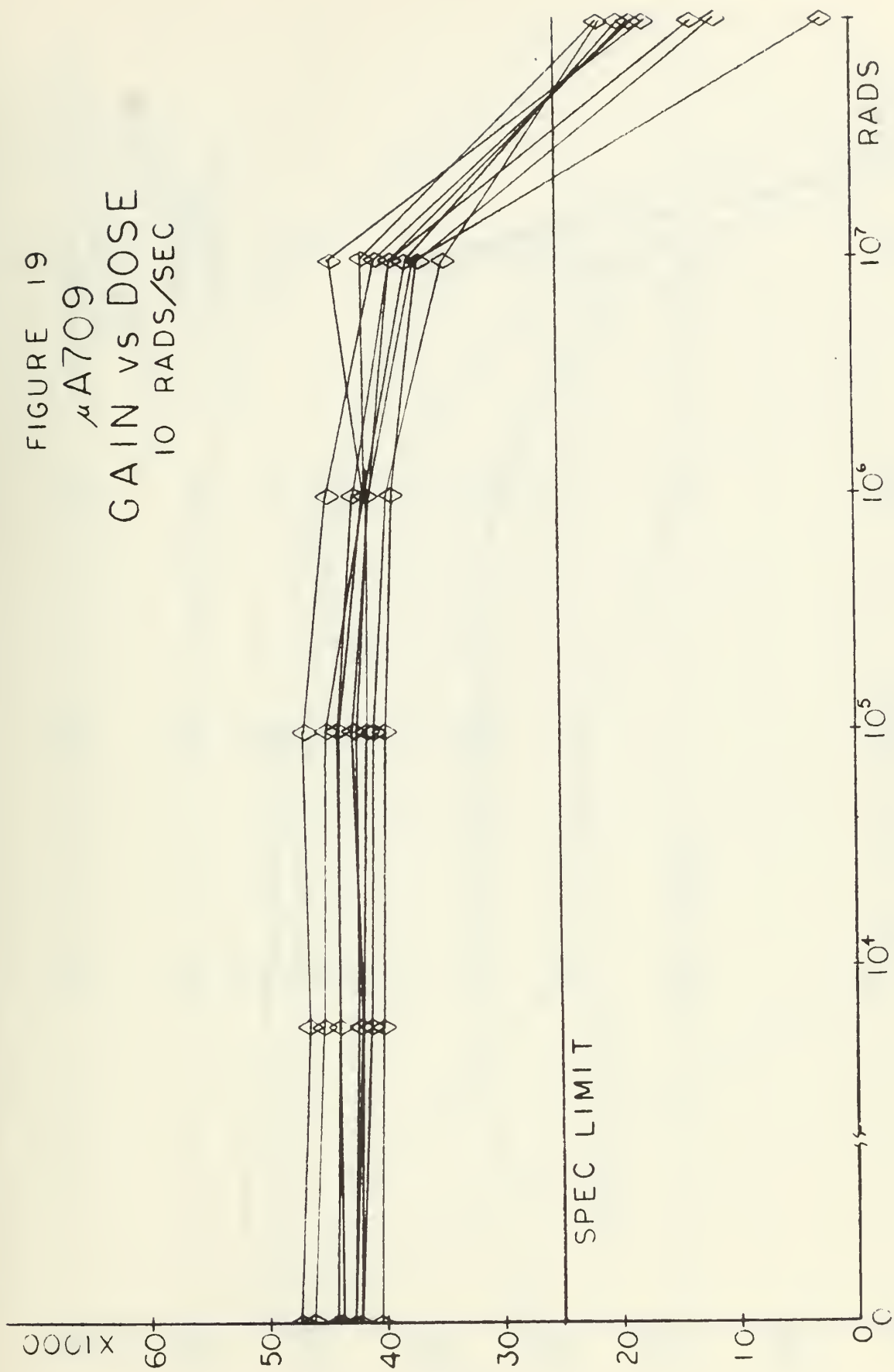


FIGURE 18
 $\mu A744$
 IBAV VS DOSE
 10^{10} RADS/SEC

FIGURE 19
 μ A709
 GAIN vs DOSE
 10 RADS/SEC



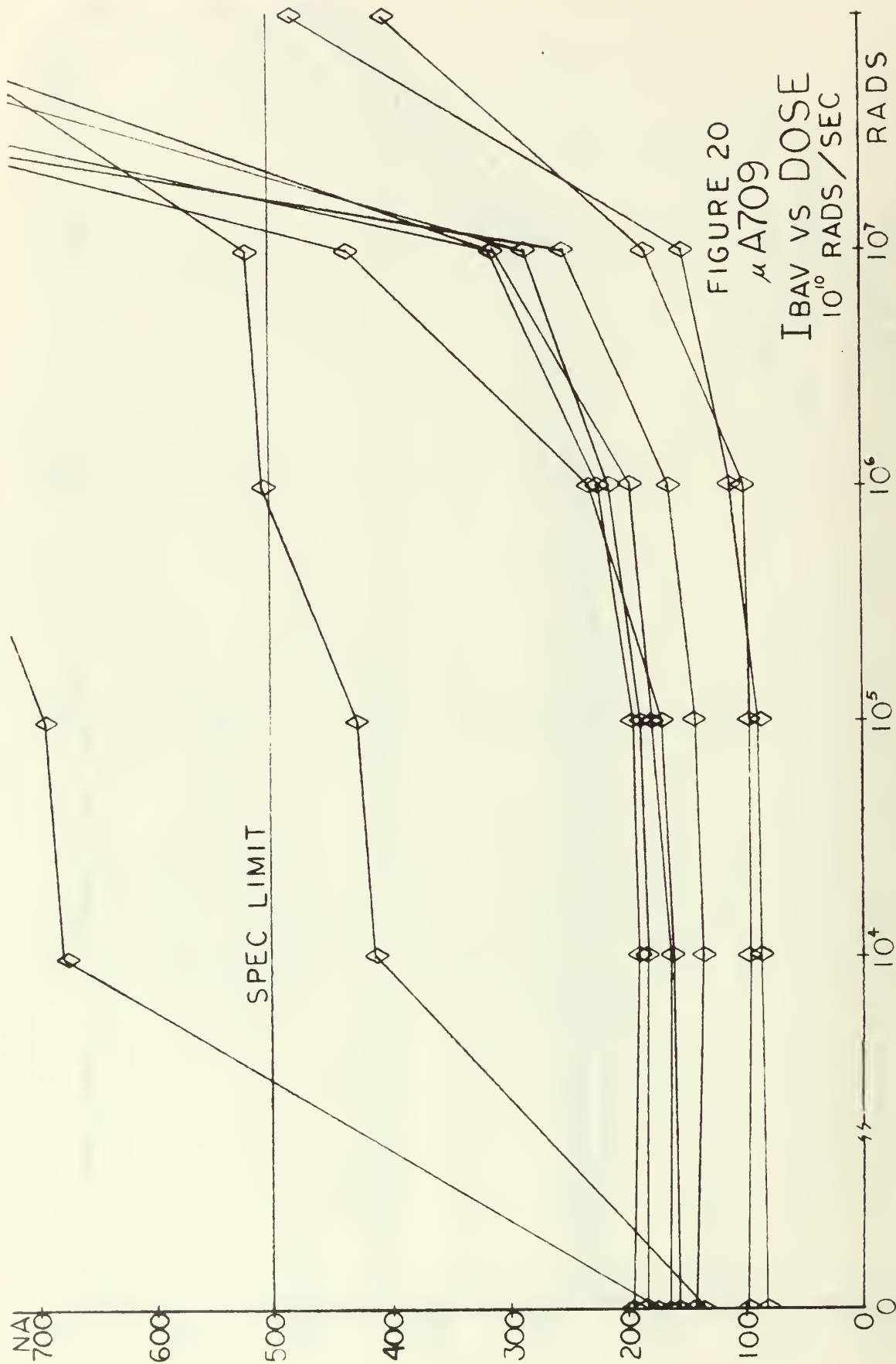
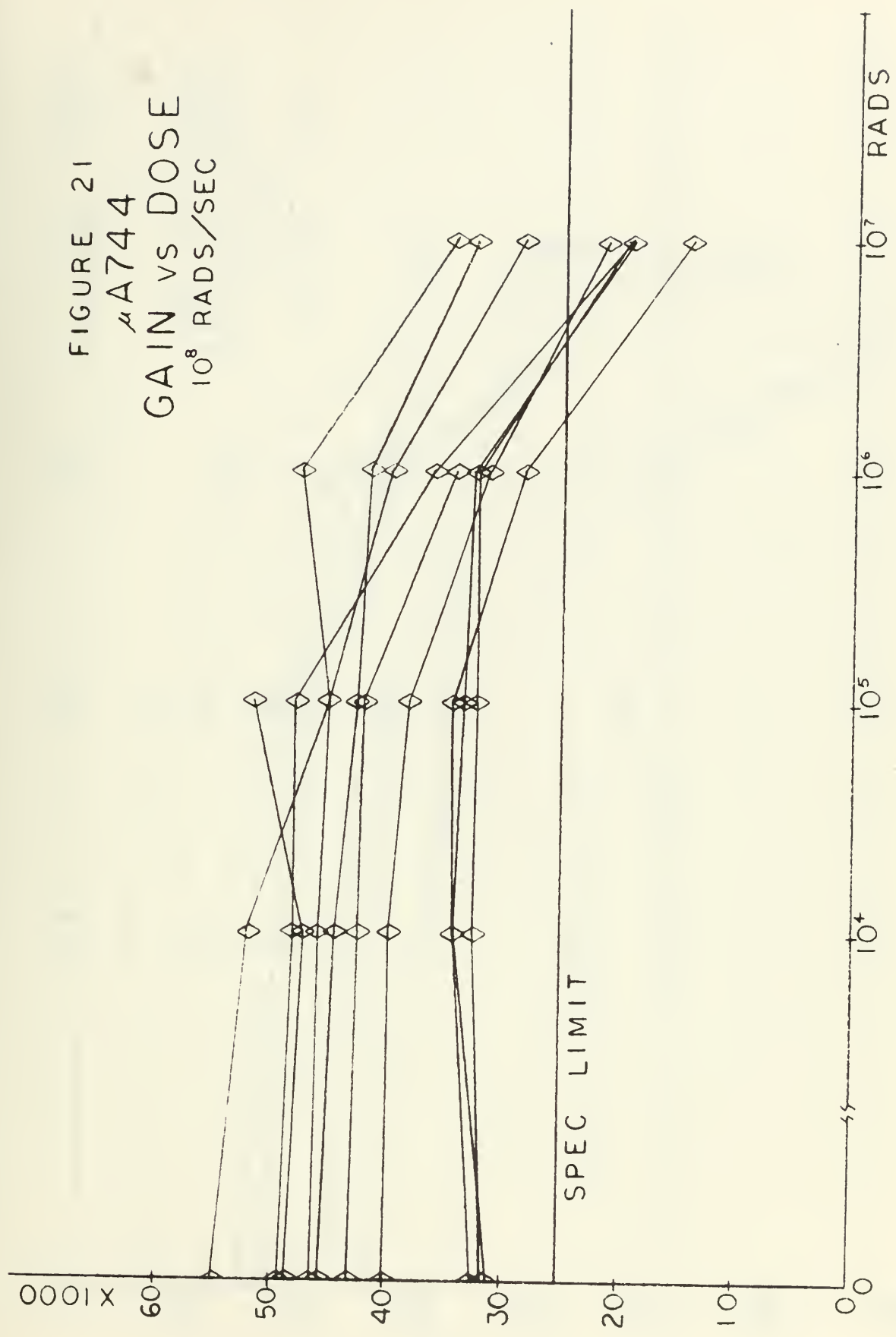


FIGURE 20
 μ A709
 IBAV VS DOSE
 10^0 RADS/SEC

FIGURE 21
 A744
 GAIN vs DOSE
 10^8 RADS/SEC



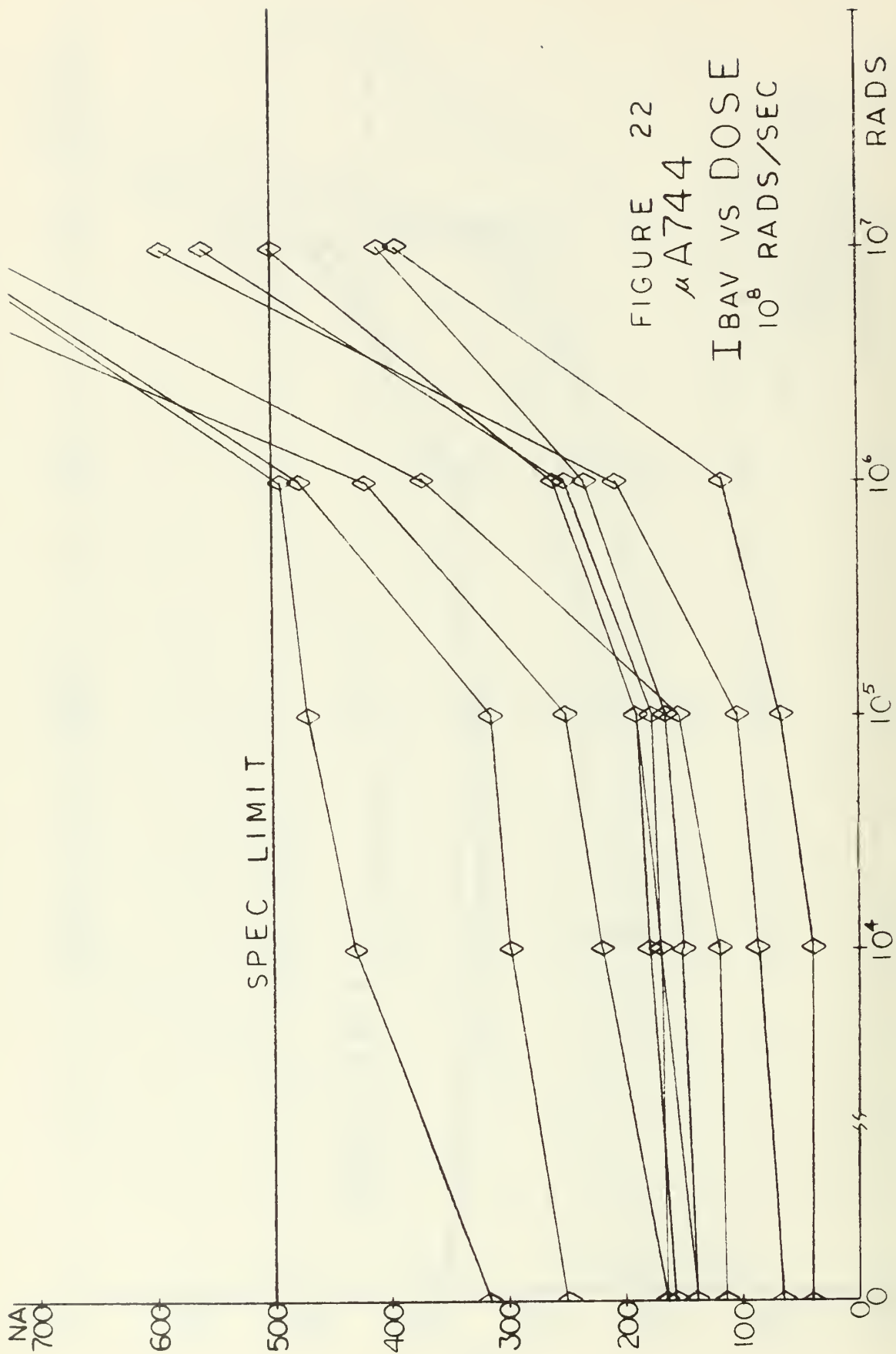
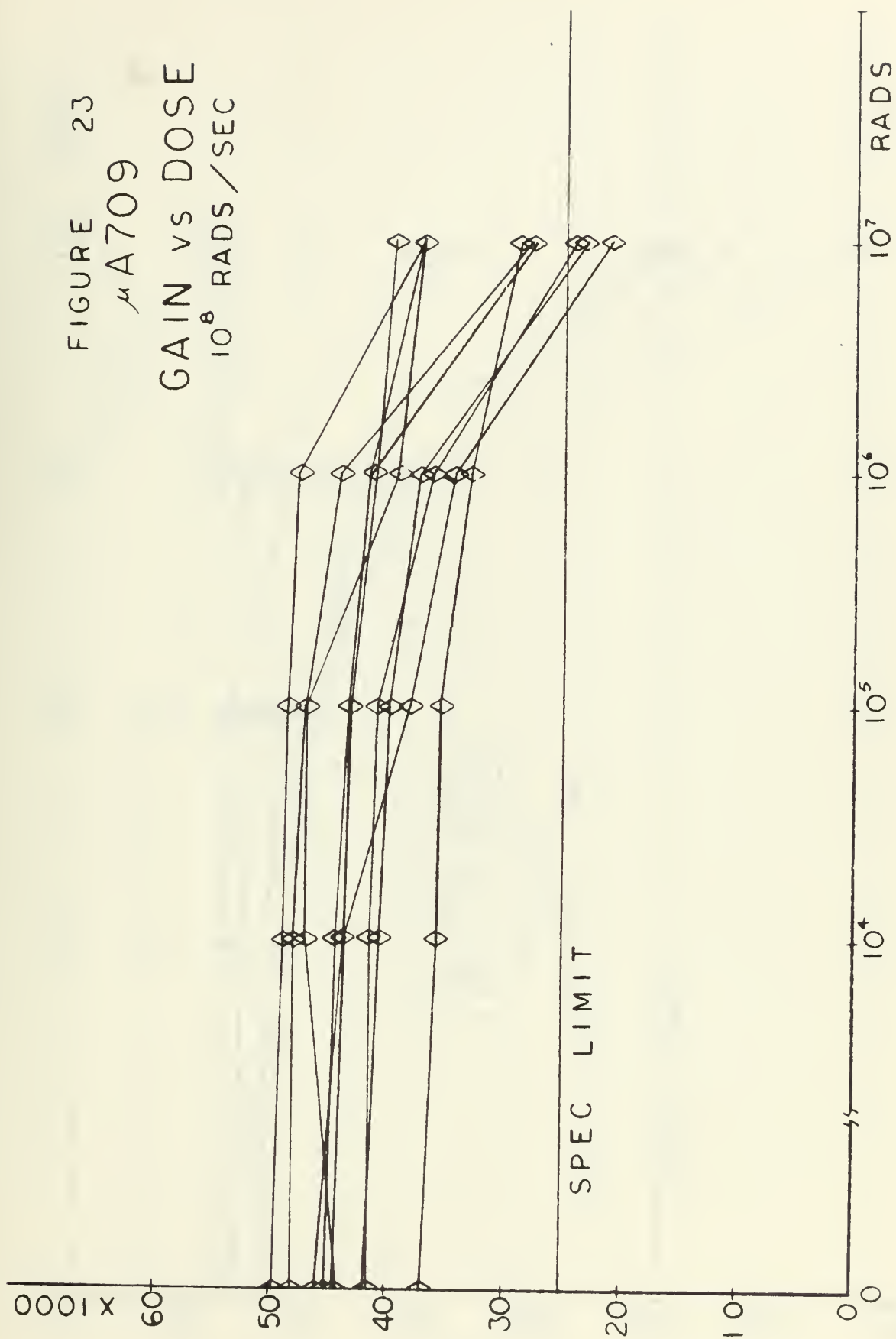


FIGURE 23
 μ A709
 GAIN vs DOSE
 10^8 RADS/SEC



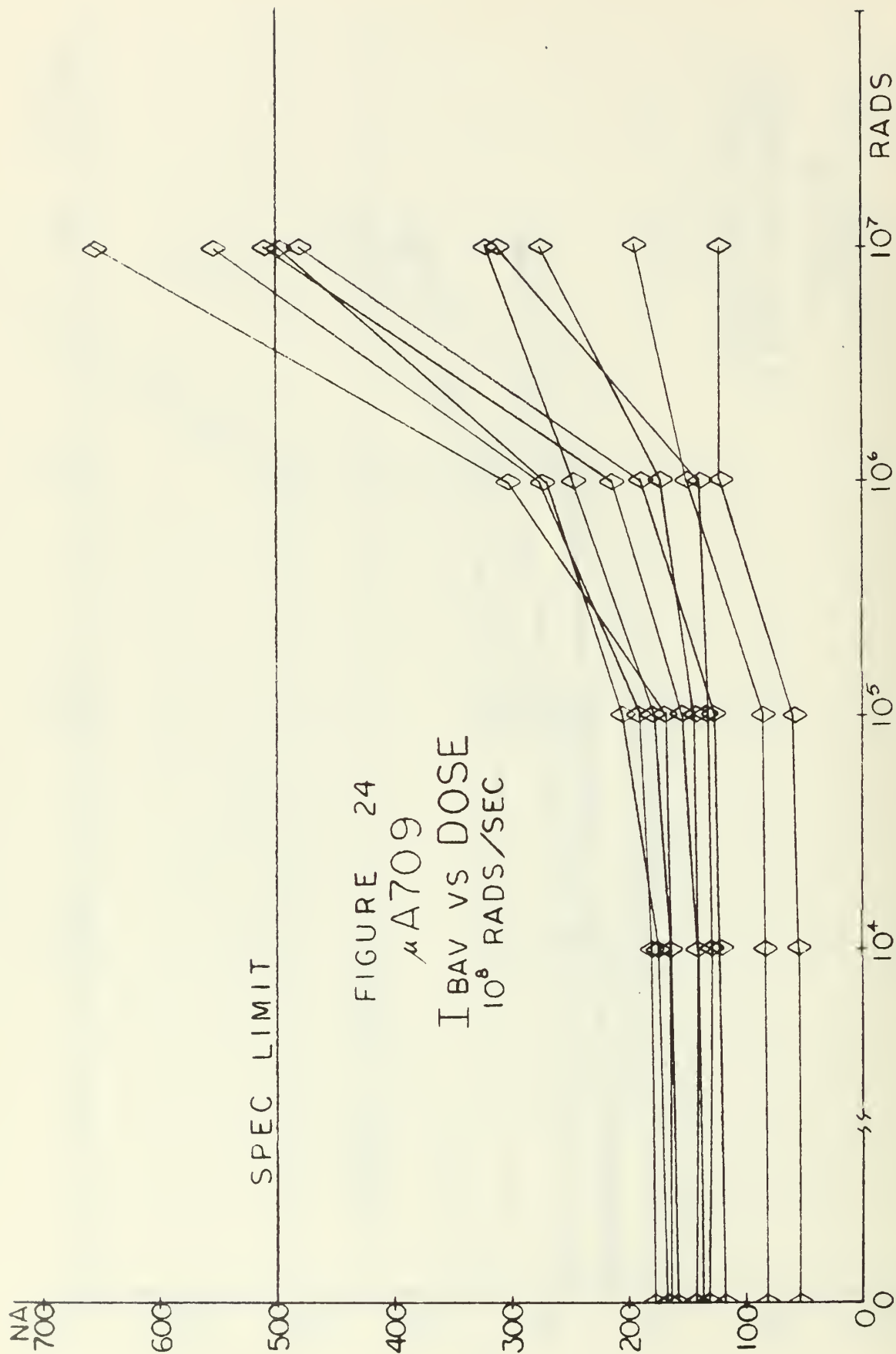
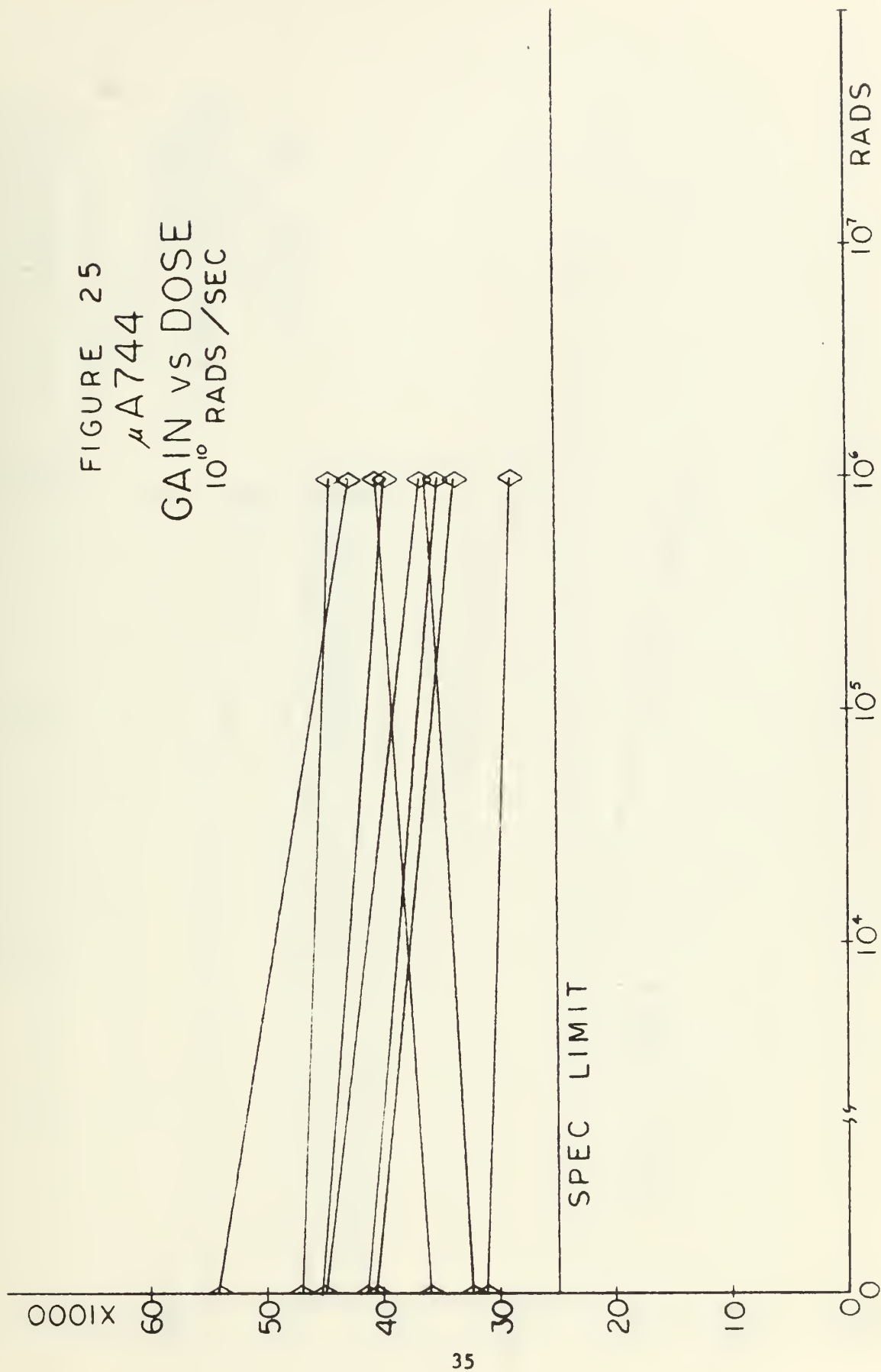


FIGURE 25
 μ A744
 GAIN vs DOSE
 10^{10} RADS/SEC



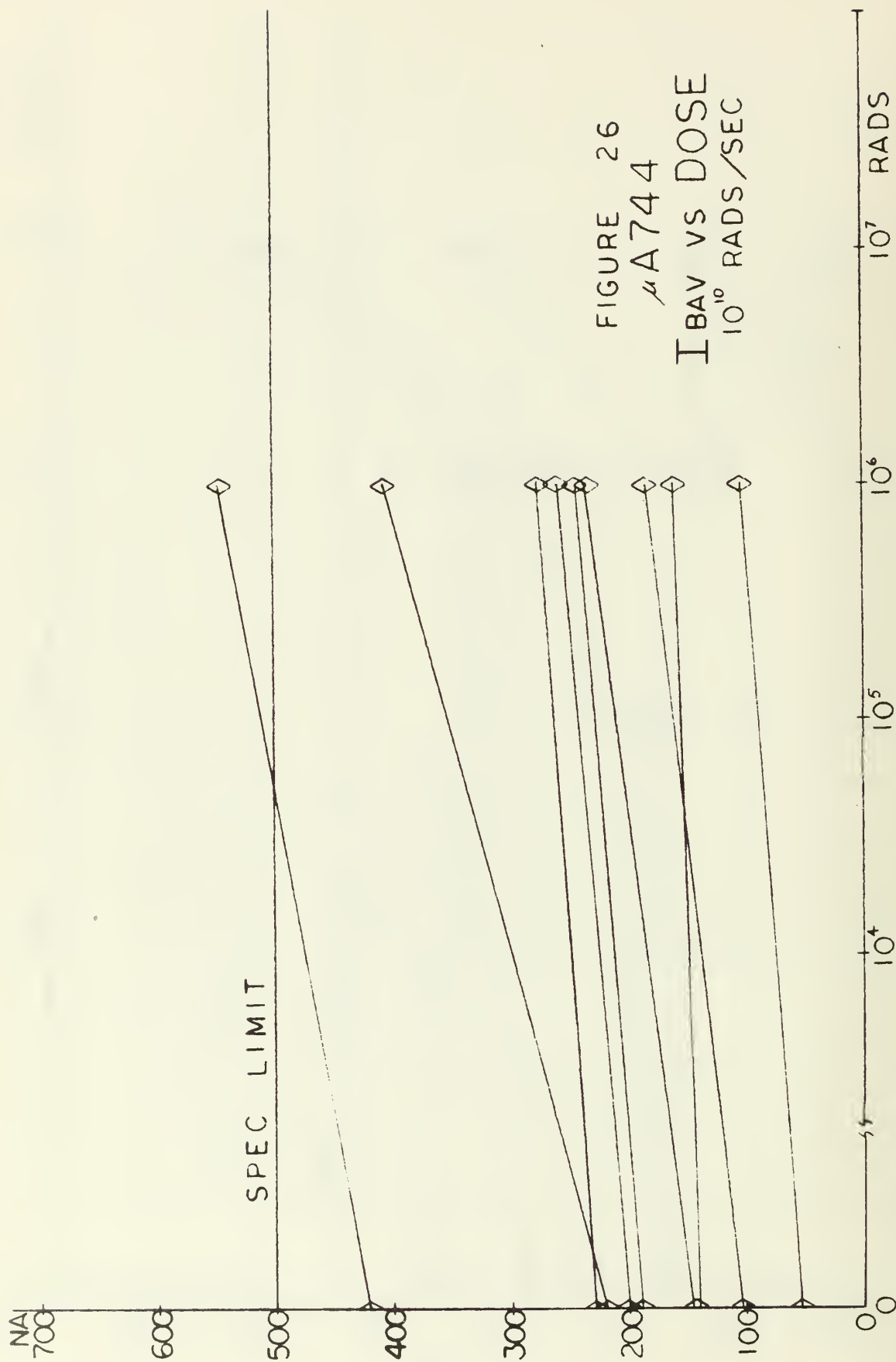
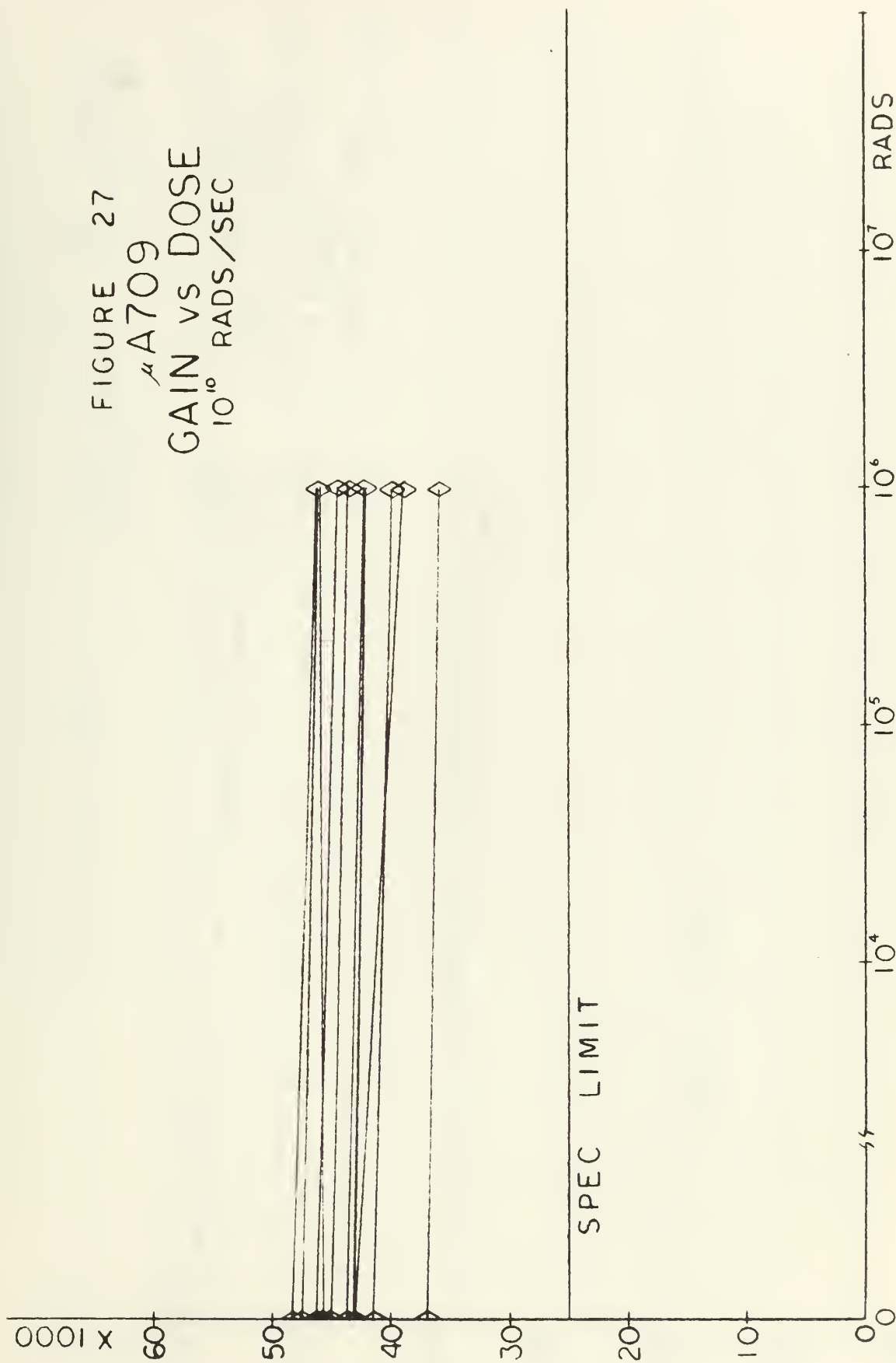


FIGURE 26
 A744
 IBAV VS DOSE
 10¹⁰ RADS/SEC

FIGURE 27
 μ A709
 GAIN vs DOSE
 10^{10} RADS/SEC



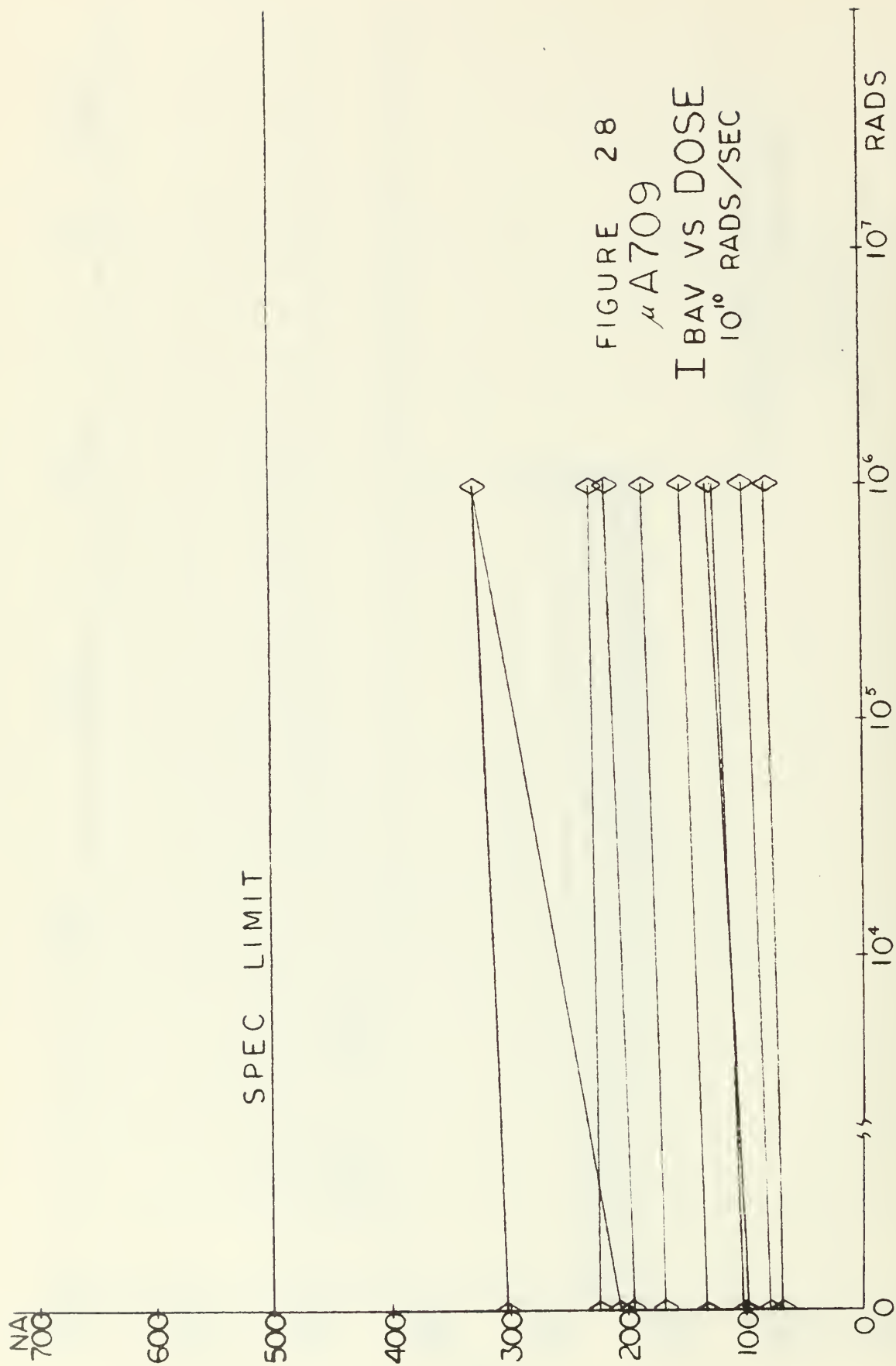
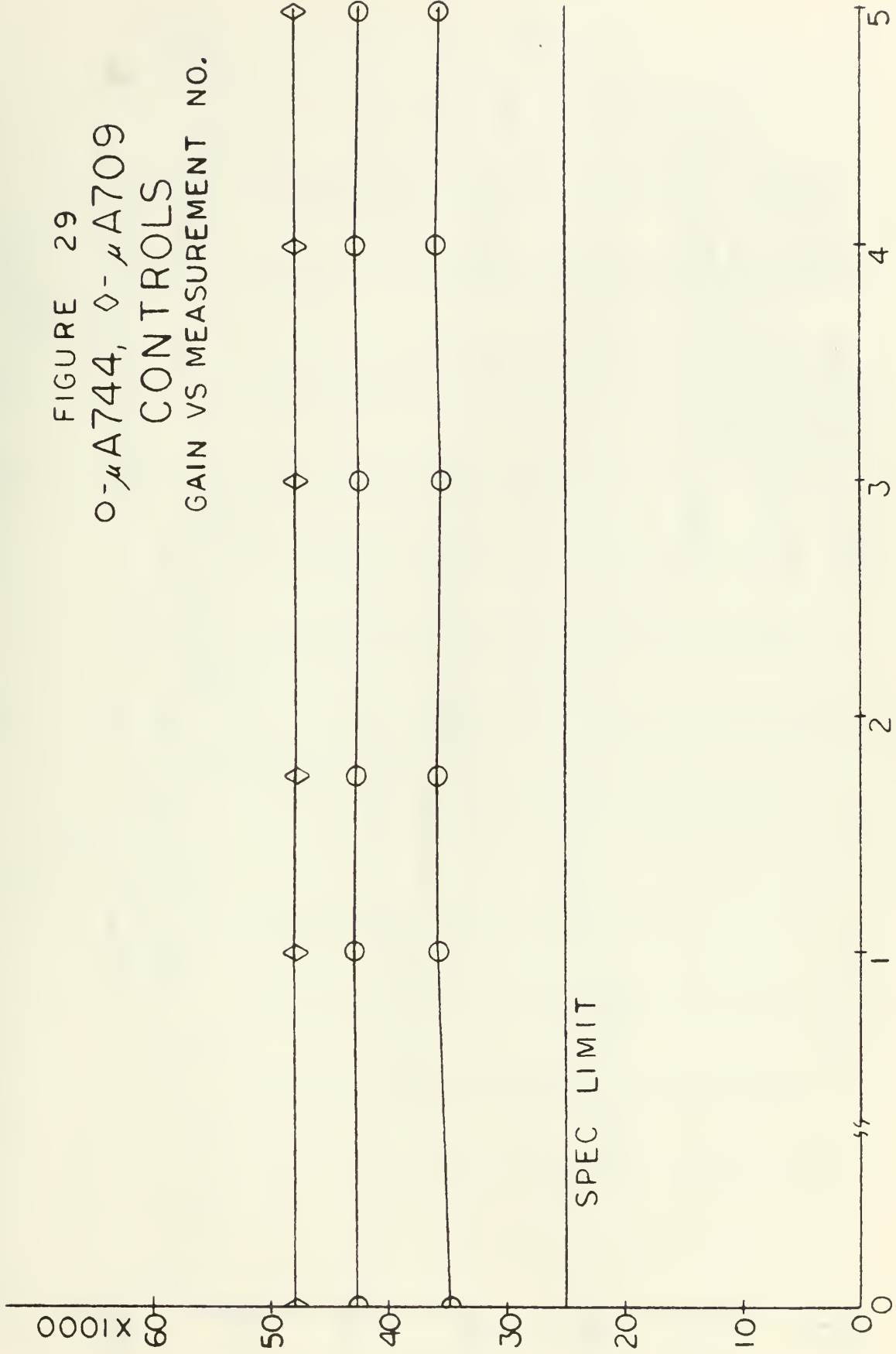


FIGURE 28
 μ A709
 IBAV VS DOSE
 10¹⁰ RADS/SEC

FIGURE 29
 $0-\mu$ A744, $\diamond-\mu$ A709
 CONTROLS
 GAIN VS MEASUREMENT NO.



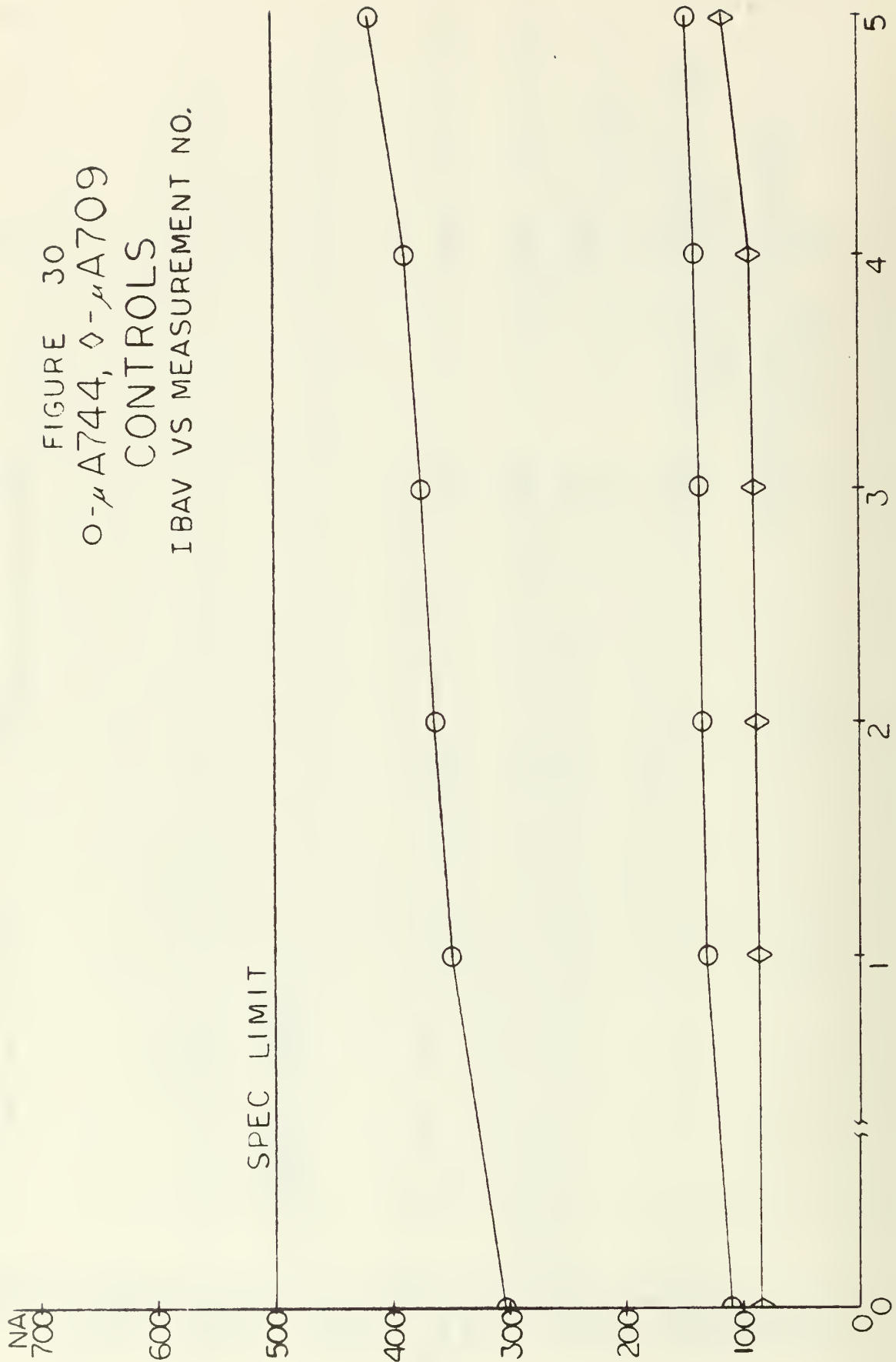


FIGURE 30
O-μ A744, δ-μ A709
CONTROLS
IBAV VS MEASUREMENT NO.

VI. CONCLUSIONS AND RECOMMENDATIONS

On the basis of the data presented, it can be concluded that the μ A744, in its present stage of development, is not more resistant to the effects of accumulated dose from high energy electrons than the μ A709.

It is recommended that a further investigation into the accumulated dose results, using kit parts, as well as continued study into the transient response of both types of circuits be the subject of a future study.

BIBLIOGRAPHY

1. Segre, E., Experimental Nuclear Physics, v. 1, p. 252, Wiley, 1953.
2. Berger, M. J. and Seltzer, S. M., Tables of Energy Losses and Ranges of Electrons and Positrons, p. 3-8, National Aeronautics and Space Administration, (NASA SP-3012), 1964.
3. Giles, J. N., Fairchild Semiconductor Linear Integrated Circuits Applications Handbook, p. 57-72, Fairchild Semiconductor, 1967.
4. MacDougall, J. S., Oberlin, D. W., and Stafford, K. R., "The Design of Radiation Hardened Integrated Circuit Operational Amplifiers," 1968 Government Microcircuit Applications Conference Digest of Technical Papers, v. 1, p. 326, October 1968.
5. Maxwell, D. A., Beeson, E. F., and Allison, E. F., "The Minimization of Parasitics on Integrated Circuits by Dielectric Isolation," IEEE Transactions on Electron Devices, v. ED-12, No. 1, p. 20, January 1965.

APPENDIX I

DOSIMETRY

Accurate dosimetry is essential for meaningful radiation damage studies. This is a difficult problem with a linear accelerator, since the electron beam has a spatial profile which must be measured.

To determine the beam distribution a number of cinemoid films were exposed. The optical density of this film changes as a function of dose. After exposure to the electron beam, the film was examined with a densitometer, and the exposure profile determined and plotted. An example is shown in Figure 32. The half-width of this curve at 0.606 of the peak is 2.1 mm. The curve can, therefore, be approximated by a Gaussian function with a standard deviation of 2.1 mm.

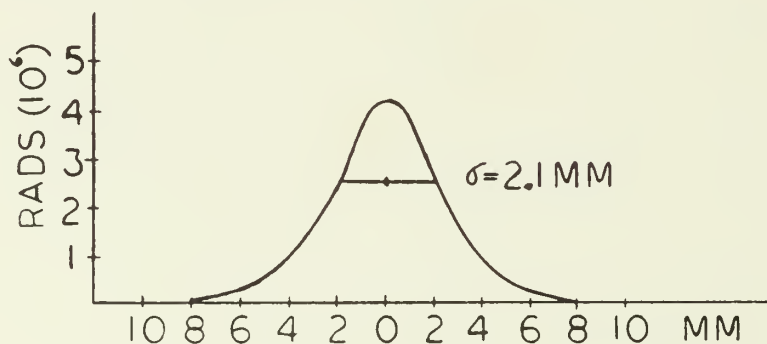


Figure 32. Beam Profile

The radial distribution of flux is therefore, $\phi(r) = \phi_0 \exp(-r^2/2\sigma^2)$ (e^-/cm^2) where ϕ_0 is the flux at $r = 0$. If N is the number of electrons, then

$$N = \int_0^\infty \int_0^\infty r \phi(r) dr d\phi = 2\pi \phi_0 \int_0^\infty r \exp(-r^2/2\sigma^2) dr = 2\pi \sigma^2 \phi_0$$

so

$$\phi_o = \frac{N}{2\pi\sigma^2} \quad \text{With } \sigma = 2.1 \text{ mm.}, \quad \phi_o = \frac{N}{0.277} = 3.6N.$$

The value of N was obtained from a Faraday cup which was assumed to be one hundred percent efficient. A measured five percent correction is necessary to allow for the scattering of electrons away from the Faraday cup by the circuits. Applying this correction, $\phi_o = 3.78N$.

Assuming that each circuit receives flux ϕ_o , the dose is given by,

$$D = \left(\frac{1}{\rho} \frac{dE}{dx} \right) \phi_o (1.6 \times 10^{-8}) \text{ rad},$$

where

$$\left(\frac{1}{\rho} \frac{dE}{dx} \right) \text{ is } 1.94 \text{ (Mevcm}^2/\text{gm)} \text{ for silicon at } 91 \text{ Mev.}$$

Finally,

$$D = 1.17 \times 10^{-7} N \text{ rad (Si).}$$

The linear accelerator is pulsed sixty times a second with a pulse duration of one microsecond. The dose rate during the pulse or the average dose rate may be obtained if the elapsed time, or the number of pulses delivered, is known.

To confirm the dosimetry calculations a PIN diode (obtained from Solid State Radiations, Inc., Los Angeles), operated at 1000 volts reverse bias, was placed in the beam. The output current from this device can be converted to dose rate in rads per sec (Si). These results were in agreement, within a factor of two, with the calculation using the Faraday cup and cinemoid films.

INITIAL DISTRIBUTION LIST

	No. Copies
1. Defense Documentation Center Cameron Station Alexandria, Virginia 22314	20
2. Library Naval Postgraduate School Monterey, California 93940	2
3. Naval Ship Systems Command (Code 2052) Department of the Navy Washington, D. C. 20360	1
4. LT D. F. Lesemann, USN DCA, 34th and Massachusetts Ave., N. W. Building 56, U. S. Naval Observatory Washington, D. C. 20305	2
5. Professor J. N. Dyer Department of Physics Naval Postgraduate School Monterey, California 93940	10
6. Professor Shu-gar Chan Department of Electrical Engineering Naval Postgraduate School Monterey, California 93940	1
7. Linear Accelerator Facility Naval Postgraduate School Monterey, California 93940	3
8. Fairchild Semiconductor R&D Lab Linear Integrated Circuits Section 4001 Miranda Blvd. Palo Alto, California 94304	6

DOCUMENT CONTROL DATA - R&D

(Security classification of title, body of abstract and indexing annotation must be entered when the overall report is classified)

1. ORIGINATING ACTIVITY (Corporate author) Naval Postgraduate School Monterey, California 93940		2a. REPORT SECURITY CLASSIFICATION Unclassified	
		2b. GROUP	
3. REPORT TITLE Comparisons between radiation hardened and standard integrated circuit amplifiers in an electron beam			
4. DESCRIPTIVE NOTES (Type of report and inclusive dates) Thesis for Master of Science Degree, April 1969			
5. AUTHOR(S) (Last name, first name, initial) Lesemann, Donald Frederick			
6. REPORT DATE April 1969		7a. TOTAL NO. OF PAGES 46	7b. NO. OF REFS 5
8a. CONTRACT OR GRANT NO.		8a. ORIGINATOR'S REPORT NUMBER(S) N/A	
A. PROJECT NO. N/A			
c.		8b. OTHER REPORT NO(S) (Any other numbers that may be assigned this report) N/A	
d.			
10. AVAILABILITY/LIMITATION NOTICES Distribution of this document is unlimited.			
11. SUPPLEMENTARY NOTES		12. SPONSORING MILITARY ACTIVITY Naval Postgraduate School Monterey, California 93940	

13. ABSTRACT

An investigation into the effect of radiation from a linear accelerator on two types of integrated circuit operational amplifiers was made. Dielectric isolation, thin film resistors and compensation diodes were used in one amplifier (μ A744). The other amplifier (μ A709) was fabricated using standard methods.

The μ A744 amplifier, in its current stage of development, was found to be more susceptible to the effects of accumulated dose from high energy electrons than the μ A709 amplifier.

KEY WORDS

LINK A

LINK B

LINK C

ROLE

WT

[illegible]

WT

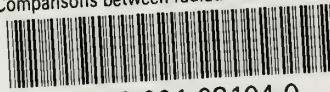
ROLE

WT

Linear Accelerator

thesL547

Comparisons between radiation hardened a



3 2768 001 03104 0

DUDLEY KNOX LIBRARY